Electronic Supplementary Material (ESI) for Nanoscale.
This journal is © The Royal Society of Chemistry 2015

Electronic Supplementary Information

A Light-driven Supramolecular Nanowire Actuator

Junho Lee,[a] Seungwhan Oh,[b] Jaeyeon Pyo,[a] Jong-Man Kim*[b,c] and Jung Ho Je*[a]

[a] X-ray Imaging Center, Department of Materials Science and Engineering, Pohang University of Science and Technology, Pohang 790-784, Korea

[b] Department of Chemical Engineering, Hanyang University, Seoul 133-791, Korea

[c] Institute of Nano Science and Technology, Hanyang University, Seoul 133-791, Korea

* e-mail: jhje@postech.ac.kr, jmk@hanyang.ac.kr

Experimental detail

Growth of the Azo-1 nanowires : *Tris*(4-((*E*)-phenyldiazenyl)phenyl)-benzene-1,3,5-tricarboxamide (Azo-1) powder was dissolved in dimethylformamide (DMF) at a concentration of 30 mM. A glass micropipette was filled with the Azo-1 solution. The micropipette (opening radius r_0 ~ 1 μm) was obtained with a pipette-puller (P-97, Sutter Instrument). The motion of the micropipette was accurately controlled by using x-y-z stepping motors, having a positioning accuracy of 250 nm (KOHZU Precision). When the micropipette touches a substrate, a meniscus of the Azo-1 solution is created outside its tip opening. As the micropipette is pulled up in vertical direction, the meniscus solution is stretched and the solvent is rapidly evaporated, resulting in Azo-1 nanowire. The procedure of the Azo-1 nanowire growth was monitored in *real-time* by using a home-built optical imaging system (Fig. S2†) which was composed of a CCD camera (Infinity *1*-2 Lumenera) coupled with an objective lens (Mitutoyo, 100x Plan Apo HR Infinity Corrected Objective). A tungsten-halogen lamp (KWANGWOO, 150 W) with a fiber-optic bundle that guided light from a sample was used as a light source. *Real-time* grazing incidence X-ray diffraction (GIXD) experiments on an Azo-1 microwire on Si (100) were performed at 5A beam line of Pohang Acceleration Laboratory (Korea). The sample was mounted on a two-axis goniometer on top of an x–z stage and the diffracted intensity was recorded by a Mar charge-coupled device detector. The incident-beam angle was 0.1° for 2D GIXD patterns.

Characterization of the actuation response: UV (λ ~ 365 nm) and visible (λ ~ 455 nm) LED sources (Mightex, High-Power LED Collimator Source) were used for the bending behavior of the Azo-1 nanowires (Fig. S2†). Each LED light source was mounted on a beam splitter (Mightex, Multi-Wavelength Beam Combiner). The distance between each light source and an Azo-1 nanowire was ~10 cm. The light intensity at the sample location was controlled in the range of 1~5 mW/cm^2 and 2~10 mW/cm^2 for UV and visible light, respectively. The microscopic characteristics of the nanowire were analyzed using field emission scanning electron microscopy (FE-SEM, PHILIPS XL30SFEG).

Image analysis: The time-series of microphotographs upon UV and visible light irradiation were acquired using a CCD camera (Infinity1-2CB) with 1600 × 1200 pixels with a frame rate of 10 fps. Image-processing steps and a circle fitting algorithm based on MATLAB were used to precisely measure the bending curvature of the Azo-1 nanowires. Flatten and Gaussian filtering were used first to remove noise from raw images. Then, binary images were obtained by thresholding the raw images (Fig. S6†). Next, the binary images were skeletonized by using a thinning algorithm provided by MATLAB. Using the circle fitting algorithm (Least Mean Square (LMS) method, specifically, Newton-Fratt Method), the bending curvature of the Azo-1 nanowire was estimated.

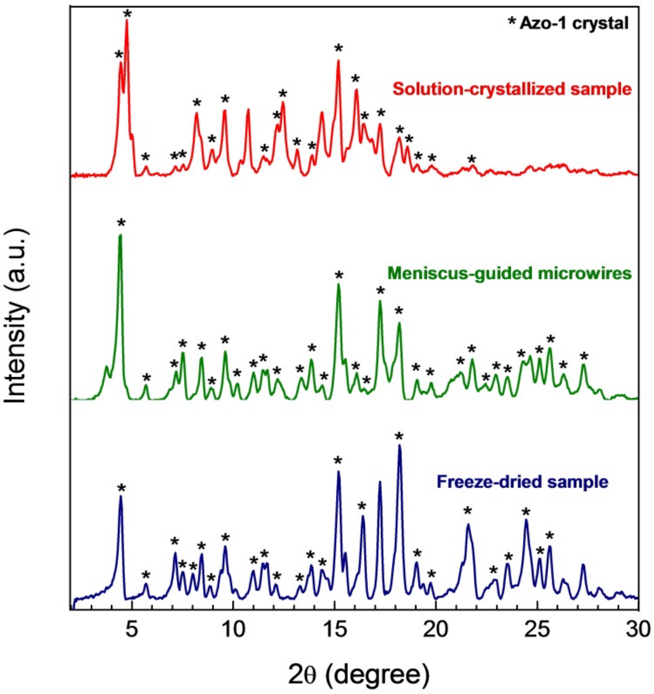

Fig. S1† X-ray powder diffraction (XRD) patterns of solution-crystallized sample, meniscus-guided microwires, and freeze-dried sample of Azo-1. All of the samples were prepared with a 20 mM DMF solution containing Azo-1. Here the solution-crystallized sample was prepared in the solution at room temperature whereas the freeze-dried sample by allowing the solvent to evaporate at -55 ºC. The microwires (20 µm in diameter) were grown by the meniscus-guided method. Not only the solution-crystallized sample and the microwires, but also the freeze-dried sample showed the diffraction peaks corresponding to the monoclinic Azo-1 crystal structure,[1] indicating a very strong crystallization behavior of Azo-1 material and suggesting that the Azo-1 nanowires grown at room temperature by the meniscus-guided method have the monoclinic crystal structure.

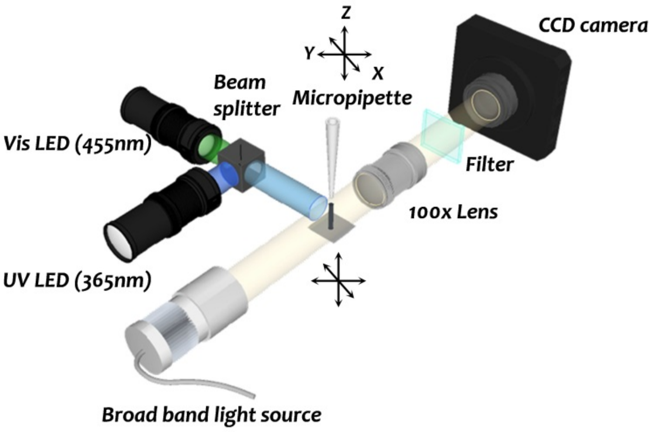

Fig. S2† Schematic representation of experimental set-up for growth of Azo-1 nanowires and characterization of the actuation response.

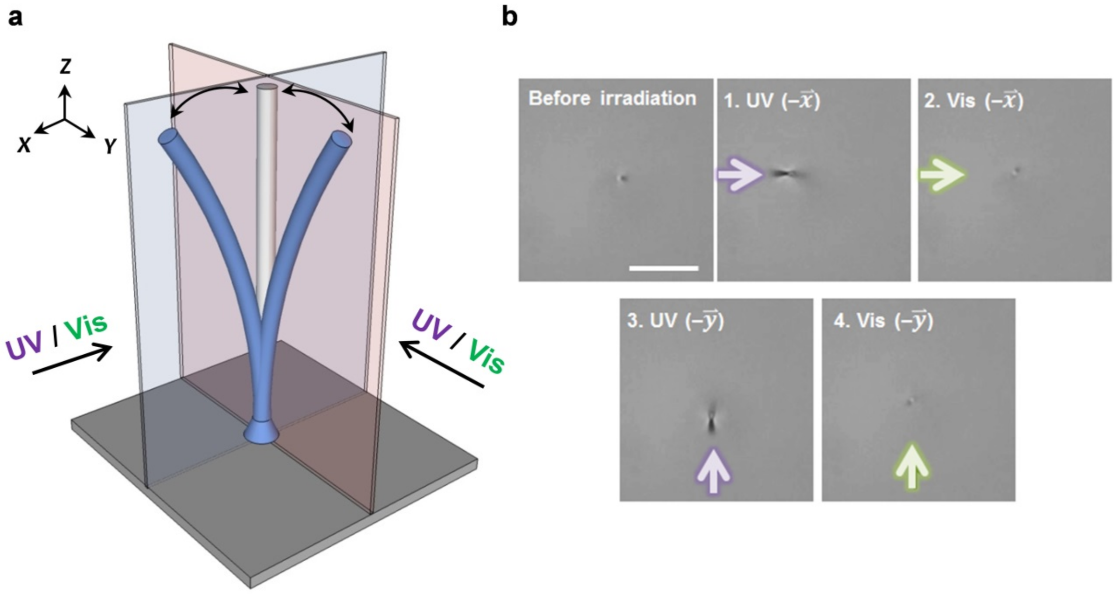

Fig. S3† (a) Schematic representation of 3D bending motion. (b) Top-view optical microscope images show 3D bending motion of an Azo-1 nanowire (500 nm (*d*) x 45 µm (*l*)). Scale bar, 20 µm.

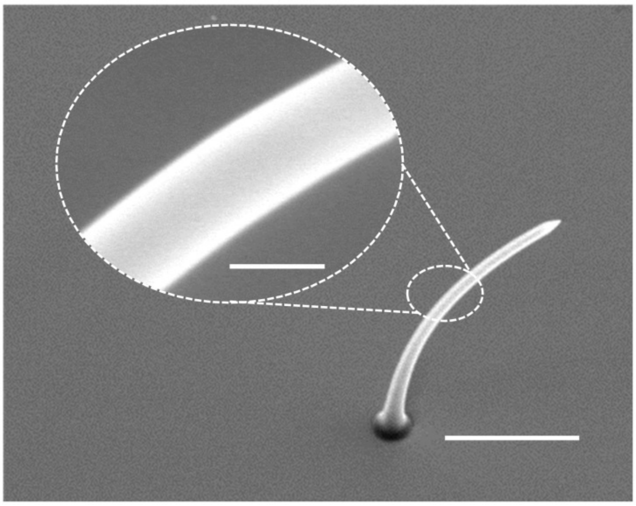

Fig. S4† FE-SEM image of a bent Azo-1 nanowire after UV irradiation. There are no cracks or fragmentation in the surface of the nanowire, due to the high surface-to-volume ratio of our nanowires that provides sufficient strain relief during the transition.[2] Scale bar, 5 μm. Inset: A higher magnification FE-SEM image of the Azo-1 nanowire. Scale bar, 500 nm.

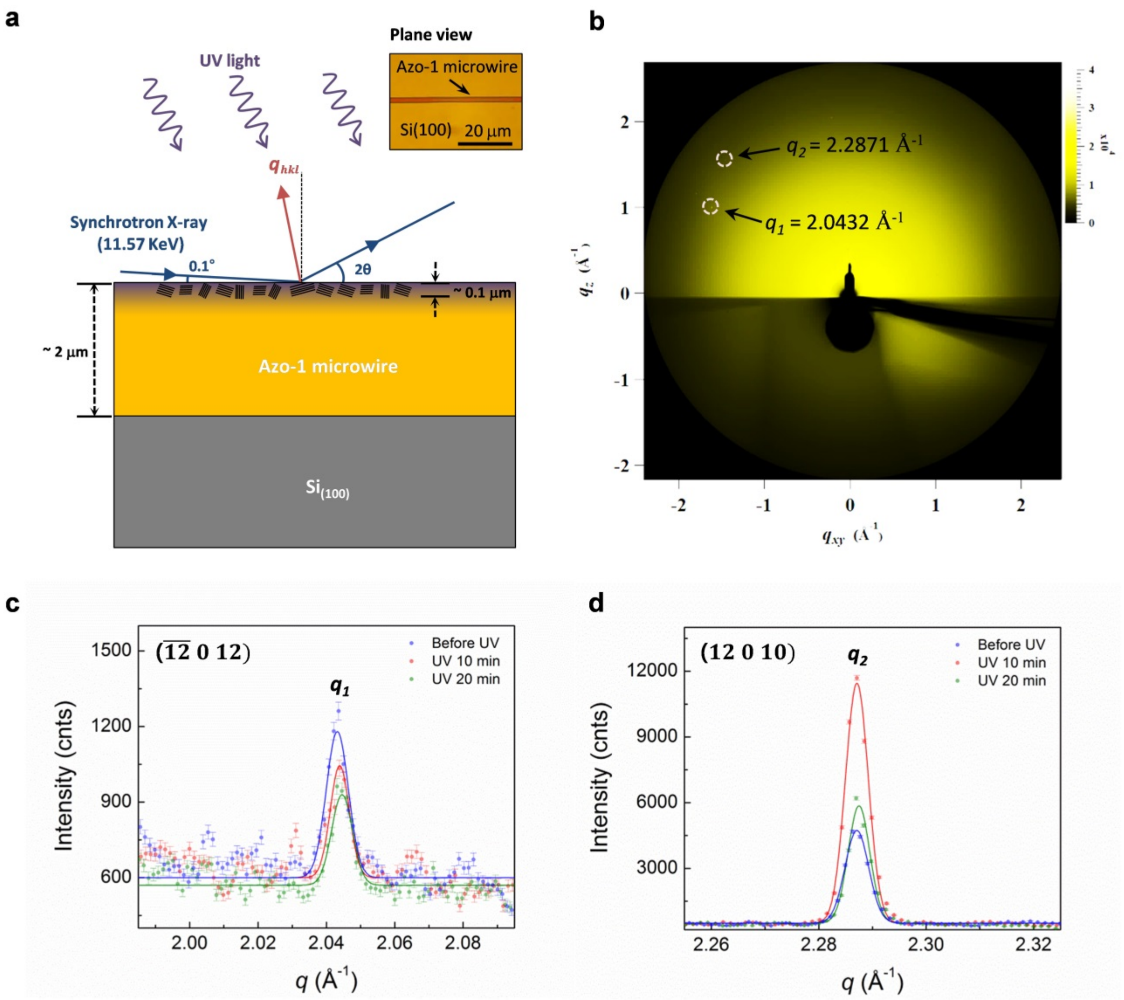

Fig. S5† (a) Experiemntal set-up of *real-time* grazing incidence X-ray diffraction (GIXD) for an Azo-1 microwire (2 μm in diameter), line-patterned on Si(100) substrate (plane view). By this total X-ray reflection condition (θ (= 0.1°) < θ_c (= 0.11°)), the penetration depth of the incident X-rays could be adjusted as ~ 0.1 μm from the Azo-1 microwire surface. (b) A two-dimensional GIXD pattern of the Azo-1 microwire before UV irradiation. By the GIXD geometry, we successfully identified two Azo-1 $(\bar{1}2\ 0\ 12)$ and (12 0 10) domains from the microwire surface region with q_1 = 2.0432 Å^{-1} and q_2 = 2.2871 Å^{-1}, respectively. (c) The Bragg peaks of the $(\bar{1}2\ 0\ 12)$ domain (q_1 = 2.0432 Å^{-1}, domain size = 40 nm, measured from the full width at half maximum (FWHM)), measured in *real-time* during UV irradiation. We find that the peak position gradually increases from q = 2.0432 Å^{-1} before UV irradiation to q = 2.0439 Å^{-1} under 10 min UV irradiation, and further to q = 2.0445 Å^{-1} under 20 min UV irradiation. This result immediately indicates that the interplanar spacing of the Azo-1 domain at the surface region gradually contracts with UV irradiation. (d) The Bragg peaks of the (12 0 10) domain (q_2 = 2.2871 Å^{-1}, domain size = 80 nm) also showed similar contraction behavior under UV irradiation. From these GIXD results, we confirmed that the Azo-1 crystal at the surface region really contracts by *trans* to *cis* conversion under UV irradiation.

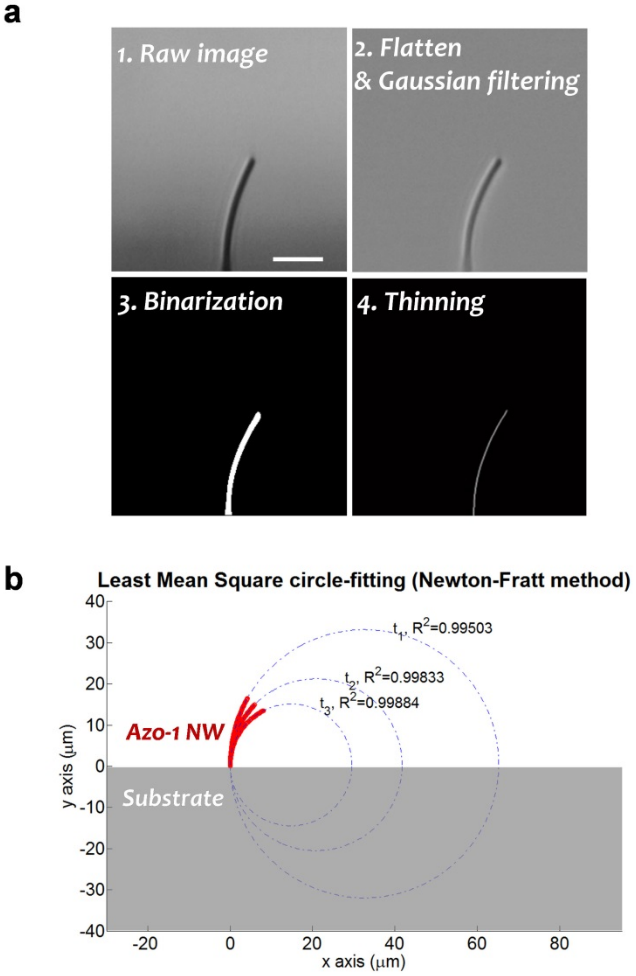

Fig. S6† Imaging analyses were performed using a series of image-processing steps and a circle fitting algorithm based on MATLAB to precisely measure the bending curvatures (*1/R*) of the Azo-1 nanowires upon UV and visible light irradiation. (a) Three image-processing steps. Scale bar, 10 μm. (b) A circle-fitting of representative time-series skeletonized images of a nanowire based on a circle-fitting algorithm (Least Mean Square (LMS) method, specifically, Newton-Fratt Method). R^2 is coefficient of determination.

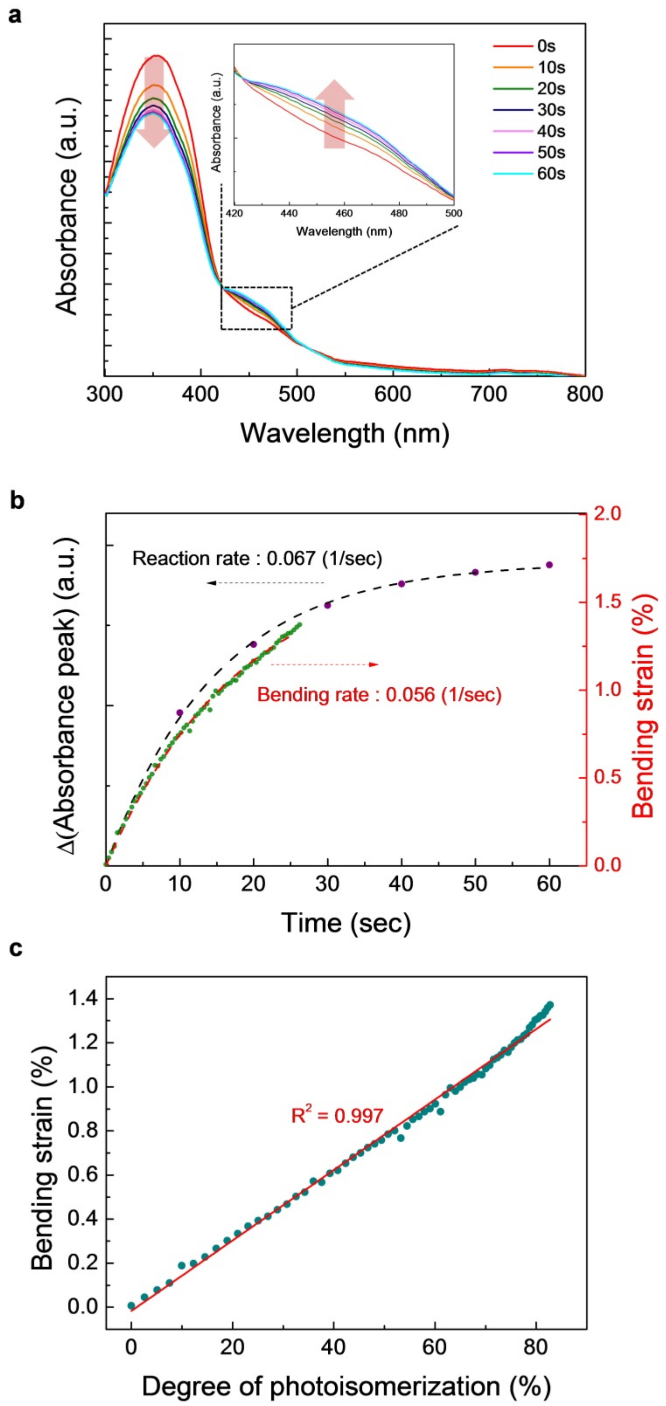

Fig. S7† (a) Absorption spectra of an Azo-1 film under UV irradiation (365 nm, 1.6 mW/cm^2) up to 60 s. Upon UV irradiation, *trans*-*cis* (E/Z) photoisomerization occurred, as seen in the gradual decrease in the intensity at 360 nm that is from the *trans* chromophores or the gradual increase in the intensity at 455 nm that is from the *cis* chromophores. The relatively slight increase in the *cis* absorbance band is due to the limited UV penetration (~ 100 nm) from the film surface. The photoisomerization of three azobenzene chromophores in Azo-1 is expected to proceed with four discrete states (EEE, EEZ, EZZ, and ZZZ) upon UV irradiation, as reported.[3] (b) The change of the absorbance peak at 365nm (left y-axis) and the bending strain of the nanowires (right y-axis) as a function of UV irradiation time. The change of the absorbance peak showed first-order kinetics of the photoisomerization in azobenzene. Here, the reaction rate (0.067/s), estimated from fitting the change of the absorbance peak at 365 nm to [$1 - \exp(-k_{\mathrm{react}}t)$], was a little larger than the bending rate (0.056/s), estimated in Fig. 4(d). (c) Plot of bending strain and degree of photoisomerization. Due to the small difference between the reaction and the bending rates in (b), the relationship between bending strain and degree of photoisomerization is almost linear ($R^2 = 0.997$).

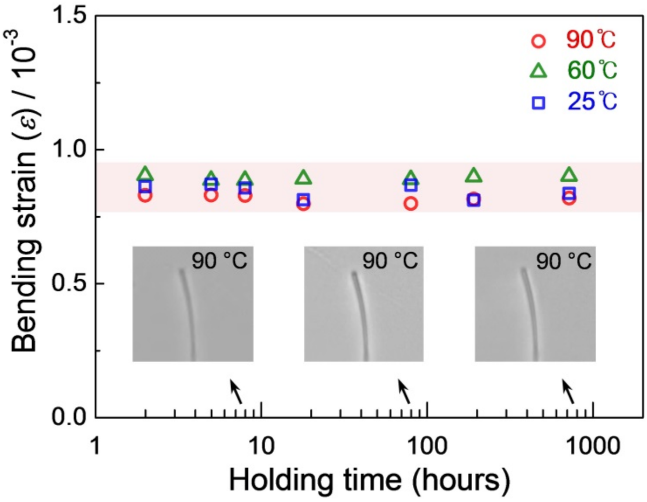

Fig. S8† The bending strains of the Azo-1 nanowires (500 nm (*d*) x 22.5 μm (*l*)), measured as a function of time at a given temperature (25, 60, and 90 ºC) after irradiation with UV light (1.6 mW/cm^2, 10 s), display little variations up to one month. (Inset) Representative optical microscope images of an Azo-1 nanowire, after 8 h, 72 h, and a month at 90 °C. The bending strains were estimated as $8.45 \times 10^{-4} \pm 0.25 \times 10^{-4}$ (average ± SEM), $8.93 \times 10^{-4} \pm 0.07 \times 10^{-4}$, and $8.17 \times 10^{-4} \pm 0.14 \times 10^{-4}$ at 25 °C, 60 °C, and 90 °C, respectively. Scale bar, 2 μm.

References

1. S. Lee, S. Oh, J. Lee, Y. Malpani, Y.-S. Jung, B. Kang, J. Y. Lee, K. Ozasa, T. Isoshima, S. Y. Lee, M. Hara, D. Hashizume, J.-M. Kim, *Langmuir*, 2013, **29**, 5869.
2. R. O. Al-Kaysi, C. J. Bardeen, *Adv. Mater.*, 2007, **19**, 1276.
3. S. Li, D. V. McGrath, *J. Am. Chem. Soc.*, 2000, **122**, 6795–6796.